Biochimica et Biophysica Acta 1858 (2016) 393–402

Contents lists available at ScienceDirect

Biochimica et Biophysica Acta

journal homepage: www.elsevier.com/locate/bbamem

The interfacial properties of the peptide Polybia-MP1 and its interaction with DPPC are modulated by lateral electrostatic attractions

Dayane S. Alvares [a], Maria Laura Fanani [b], João Ruggiero Neto [a,*], Natalia Wilke [b,*]

[a] UNESP — São Paulo State University, IBILCE, Department of Physics, São José do Rio Preto, SP, Brazil
[b] Centro de Investigaciones en Química Biológica de Córdoba (CIQUIBIC-CONICET), Departamento de Química Biológica, Facultas de Ciencias Químicas, Universidade Nacional de Córdoba, Argentina

ARTICLE INFO

Article history:
Received 17 September 2015
Received in revised form 16 November 2015
Accepted 4 December 2015
Available online 7 December 2015

Keywords:
Peptide–peptide lateral interactions
Langmuir-monolayer
Lipid–peptide co-crystals
Domain shape
Membrane electrostatic interactions

ABSTRACT

Polybia-MP1 (IDWKKLLDAAKQIL-NH2), extracted from the Brazilian wasp *Polybia paulista*, exhibits a broad-spectrum bactericidal activity without being hemolytic and cytotoxic. In the present study, we analyzed the surface properties of the peptide and its interaction with DPPC in Langmuir monolayers. Polybia-MP1 formed stable monolayers, with lateral areas and surface potential values suggesting a mostly α-helical structure oriented near perpendicular to the membrane plane. In DPPC–peptide mixed monolayers, MP1 co-crystallized with the lipid forming branched domains only when the subphase was pure water. On subphases with high salt concentrations or at acidic or basic conditions, the peptide formed less densely packed films and was excluded from the domains, indicating the presence of attractive electrostatic interactions between peptides, which allow them to get closer to each other and to interact with DPPC probably as a consequence of a particular peptide arrangement. The residues responsible of the peptide–peptide attraction are suggested to be the anionic aspartic acids and the cationic lysines, which form a salt bridge, leading to oriented interactions in the crystal and thereby to branched domains. For this peptide, the balance between total attractive and repulsive interactions may be finely tuned by the aqueous ionic strength and pH, and since this effect is related with lysines and aspartic acids, similar effects may also occur in other peptides containing these residues in their sequences.

1. Introduction

Helical antimicrobial peptides are short sequences, up to 50 amino acids, rich in cationic, non-polar and hydrophobic residues, whose distribution along the chain allows the formation of an amphipathic helix when in membrane. Thanks to their cationicity, these peptides have selective preference for anionic lipid membranes, which is the main characteristic of the outer leaflet of prokaryotic plasmatic membranes [1]. Diverse studies have demonstrated that their efficiency of action against anionic membrane is strongly dependent on the membrane properties and the peptide structural features as net charge, charge distribution and hydrophobicity [1–3]. These peptides display, in general the ability to disturb lipid bilayers inducing leakage of the cell content. Several models have been proposed for the mechanism of action of these peptides and they have been extensive and comprehensibly described in a recent review [4]. These mechanisms are not exclusive and some peptides can display more than one depending on the peptide-to-lipid ratio. These models suggest that their disturbance on the lipid packing induces leakage without requiring specific membrane receptor [5]. By this ability in acting only on the lipid phase of the membrane, these peptides have a great potential to substitute conventional antibiotics [1] or as a model to the design of new drugs based on the membrane as their main target. The search for new compounds with antimicrobial activity has been very active in the last two decades due to the increase in the number of bacterial strains resistant to the conventional antibiotics [1] that is considered as one of the greatest health public problem of this century. Studies have also shown that, besides their antimicrobial activities these peptides also can act against cancer cells [6].

Polybia-MP1 (IDWKKLLDAAKQIL-NH2), or simply MP1, is an example of these peptides. It is extracted from the venom of the Brazilian wasp *Polybia paulista* and exhibits a broad-spectrum bactericidal activity without being hemolytic and cytotoxic [7]. MP1 also showed a selective inhibitory effect on proliferating prostate and bladder cancer cells [8], and against multidrug-resistant leukemic cells [9]. In addition, this peptide is cytotoxic against leukemic T lymphocytes and highly selective in recognizing these cells compared with healthy lymphocytes [10].

An important feature of this peptide is the presence of two aspartic acids concomitantly with three lysines and the amidated C-terminus, conferring a low positive net charge (+2e) at physiological pH values. This low net charge, however, does not hamper its selectivity to anionic bilayers in comparison to zwitterionic ones. Studies of the peptide interaction with model membranes were used to investigate the physico-

* Corresponding authors.
E-mail addresses: jruggiero@sjrp.unesp.br (J. Ruggiero Neto), wilke@fcq.unc.edu.ar (N. Wilke).

http://dx.doi.org/10.1016/j.bbamem.2015.12.010
0005-2736/

chemical bases for its affinity to membranes. It was observed that the adsorption of the peptide to large unilamellar vesicles is coupled to its folding to a helical conformation. We also demonstrated that the D2 residue plays an important role in modulating the affinity of MP1 for zwitterionic (POPC) and mixed POPC:POPG (7:3) anionic vesicles [11,12]. Molecular dynamics simulation in trifluoroethanol (TFE) showed that the acidic residues are paired with positive residues: D2 with N-terminus and K5 and D8 with K4 and K11 [12] confirming an important role of the D2 residue as well as the distribution of the charged residues on the energetic balance for a helical structure in PC vesicles [13]. MP1 displays higher affinity to anionic vesicles compared to other peptides with higher positive charge, in spite of the less favorable electrostatic contribution, suggesting an extra energetic component that contributes to its higher affinity [13].

The interfacial properties of MP1 are believed to play an important role in its interaction with lipid membrane. In addition to the strong preference for anionic bilayers, which are due to electrostatic and non-electrostatic interactions, and translates into a potent antimicrobial activity, MP1 is not hemolytic or cytotoxic. This peptide is also able to absorb into zwitterionic POPC membranes and to induce leakage in these membranes [12]. PC is one of the most abundant phospholipids in the outer leaflet of eukaryotic cells [14] and the knowledge of this interaction will be helpful in understanding the selectivity.

To get an insight on this interaction, we explored here the surface activity of antimicrobial peptide MP1 and the lateral interactions with lipids in different conditions using Langmuir monolayers as model membranes [15]. We explored the physicochemical properties of Polybia-MP1 organized in Langmuir films and its interaction with phospholipid monolayers, composed by 1,2-dipalmitoyl-sn-3-glycerophosphocholine (DPPC). Using a neutral lipid, the non-coulombic lipid–peptide interactions can be studied and, since these interactions will also be present when the peptide is mixed with charged lipids (though coupled with stronger electrostatic effects) the results found here may help in the understanding of the global peptide–lipid interaction. It is important to remark that even for neutral lipids, electrostatic interactions may still be present since the peptide is charged and the lipid is a dipole.

Thermodynamic information was obtained from compression isotherm measurements and the surface morphology of the lipid monolayer was monitored with Brewster Angle Microscopy (BAM) and Atomic Force Microscopy (AFM). BAM is a potent tool to visualize nucleation and segregation as well as the anisotropy of microdomains as they grow at the air–water interface with a micrometer resolution in the monolayer plane [16]. AFM shows a better resolution in the plane of the film (in nanometer scale), in films supported on solid surfaces, allowing the observation of nanodomains [17]. Using AFM in association with BAM we were able to obtain detailed structural data of the film.

DPPC presents a phase transition from liquid-expanded to liquid-condensed state (LE–LC) at a surface pressure of 5 mN/m and 20 °C, therefore, we explored the effect of the presence of the peptide on the different phases of the lipid monolayers. On neutral subphases, DPPC is zwitterionic while MP1 is partially protonated. In order to explore the electrostatic properties of the peptide–lipid mixed films, the effect of ionic strength was analyzed using different ionic conditions (from 0 to 150 mM salt) and different salts (NaCl and NaBr). Experiments at acidic and basic pHs were also performed: films were prepared on solutions at pH 2.0 (where the peptide is totally protonated), pH 4.0 and pH 10.0 (where it is partially deprotonated) in order to study the effect of changes in the net charge of the peptide.

2. Materials and methods

2.1. Chemicals and reagents

1,2-Dipalmitoyl-sn-3-glycerophosphocoline (DPPC) was purchased from Avanti Polar Lipids (Alabaster, AL, USA). The lipid was used without further purification. The peptide Polybia-MP1 (MP1) was from BioSynthesis (Lewisville, TX, USA) with RP-HPLC purity level >98%. Chloroform and methanol, HPLC grade, were obtained from Merck (Darmstadt, Germany). Sodium chloride and sodium hydroxide were from Sigma Aldrich. Sodium bromide from Anedra and HCl from Merck, all these reagents were analytical grade. Ultrapure water (Millipore Milli-Q system, ~18 MΩ cm) was used for the preparation of the subphases.

2.2. Peptide solutions

The peptide was dissolved in methanol [18] and the concentration was determined from the UV absorption spectrum at 280 nm using a molar absorptivity coefficient 5570 M^{-1} cm^{-1} [19]. The spectra were collected with a spectrophotometer Varian 2300 (Palo Alto, CA, USA).

2.3. Monolayer measurements

Compression isotherms of peptide, lipid or lipid/peptide mixtures were carried out in a Teflon trough (volume 180 mL, surface area 243 cm^2) containing water or saline solutions. Surface pressure (π) was determined using a Pt plate by the Wilhelmy method, and the total film area was continuously registered using a KSV Minitrough apparatus (KSV, Helsinki, Finland) enclosed in an acrylic box. Pure peptide monolayers were prepared by spreading a solution of the peptide in methanol onto the surface of a water or saline subphase by using a microsyringe Hamilton (Reno, NV, USA). The compression isotherms of the peptides were performed at a compression rate of 0.2–0.5 $Å^2$ $molecule^{-1}$ s^{-1}, i. e., 7–20 mm/min. Surface potential-area (ΔV-A) and (π-A) isotherms were recorded simultaneously; the surface potential was determined using the Kelvin method with a KSV apparatus (KSV, Helsinki, Finland).

For lipid or lipid–peptide mixed monolayers, phospholipids were dissolved in chloroform/methanol (2:1 (v:v)) to a final concentration of 2.5 mM. Small drops of solutions of lipid or lipid–peptide premixed at a desired ratio were directly spread on the surface. The organic solvents were allowed to evaporate for 10 min before compression; monolayers were compressed at 7 mm/min. All measurements were performed at 20 °C. The determined mean molecular areas were highly reproducible, with standard deviations lower than 3% as obtained from at least three compression isotherms for each condition.

2.4. Analysis of isotherms

The mixing behavior of the lipids and the peptides was analyzed by comparing the mean molecular area of the mixture with that of an ideal mixture calculated as [20]:

$$A_{12} = A_1X_1 + A_2X_2 \quad (1)$$

where X_1 and X_2 are the molar fractions of component 1 (lipid) and component 2 (peptide), respectively, and A_1 and A_2 are the mean molecular areas of components 1 and 2 at a given surface pressure. For ideal behavior, the variation of the mean molecular area with the mole fraction of each component results in a linear relationship.

2.5. Brewster Angle Microscopy (BAM)

Langmuir monolayers were prepared as described above in the trough of a KSV Langmuir balance mounted on the stage of a Nanofilm EP3 Imaging Elipsometer (Accurion Goettingen, Germany), working in the Brewster Angle Microscopy (BAM) mode. Minimum reflection was set with a polarized laser (λ = 532 nm) incident on the bare aqueous surface at the experimentally calibrated Brewster angle (~53.1°). After monolayer formation and during compression, the reflected light was collected through a 20× objective. Further image analysis was performed using the NIH free software Image J. For better visualizing the

images, the gray level range was reduced from an original range of 0–255 to 0–80 for lipid and lipid/peptide images and to 0–40 for peptide images. The calculation of the percentage of each coexisting phase was carried out as detailed in the supporting section of Caruso et al. [21].

2.6. Atomic Force Microscopy (AFM)

The transferred monolayers were prepared as detailed in Mangiarotti et al. [22] Briefly, the hydrophilic substrates (glass coverslips) were treated with piranha solution (H_2SO_4:H_2O_2 3:1 *v*/*v*) at 90 °C for 60 min and rinsed with Milli-Q water. Then, a solution of DPPC and MP1 (7.2 mol% of MP1) was spread onto water and compressed up to 15 mN/m. The monolayer was kept at this pressure for ~200 s in order to check the absence of leakage or rearrangements, and then, since the area remained constant, the film was transferred by the Langmuir–Blodgett technique to the previously submerged substrate (oriented perpendicular to the trough) at a rate of 5 mm/min, while maintaining the surface pressure constant. Transfer ratio in the range of 1.14 (±0.10) were obtained. The supported monolayers remained in air during the surface scanning with an AFM Innova atomic force microscope (Bruker, Billerica, Massachusetts) in the tapping mode, using a silicon probe with a nominal spring constant of 40 N/m and a resonance frequency of 300 kHz at room temperature (~20 °C).

3. Results and discussion

3.1. Peptide monolayers

Fig. 1A shows the compression isotherms for films of the peptide Polybia-MP1 at the air–water interface. The peptide formed stable monolayers, as demonstrated by the compression-expansion cycles (see Fig. 1A). When the film was compressed up to low surface pressures, the recompression isotherm was similar to the compression one; as an example, the results for compressions up to 8 mN/m are shown in Fig. 1A (open squares). However, when the cycle was performed up to high surface pressures (~17 mN/m), the second compression shifted to lower areas, evidencing an irreversible loss of the peptide to the subphase at these pressures (Fig. 1A, lines).

The organization of monolayers composed of pure peptide at the micron scale was studied by imaging the surface with BAM while compressing. The images registered on pure water showed a homogeneous film in the whole range of surface pressures (see insets in Fig. 1A). The gray level of the images increased as the film was compressed, suggesting an increase in the film thickness [23].

The surface pressure increased smoothly until it reached a plateau at about 17 mN/m. This kind of plateau in the compression isotherms of peptides has been previously assigned to the formation of a bilayer [24,25] or to the collapse of the monolayer with exclusion of the material to the subphase [15,26]. For films of MP1, once the plateau was reached, the gray level in the BAM images also reached a maximal value, and this value remained constant upon further compression (see the open circles in Fig. 1A). This result along with the shift to lower areas displayed in the compression-expansion cycles indicate that for MP1 films, the plateau at 17 mN/m corresponded to the collapse of the film.

The effect of salt on the compression isotherms of the peptide films was analyzed by spreading the peptide on saline solutions at neutral pHs. Fig. 1B compares the compression isotherms (surface potential and surface pressure vs mean molecular area) of films of MP1 on water and on a 150 mM NaCl solution (pH 7.4). The peptide formed stable monolayers also on salt solutions, as evidenced by a high similitude in the isotherms obtained with compression-expansion cycles (data not shown). Regarding the film topography on NaCl solutions, the BAM images of this system showed a trend similar to that observed on water (see Fig. 1A). In the presence of salt, the isotherms shifted to higher areas and the plateau corresponding to collapse was about 21 mN/m (Fig. 1B). Similar features have been observed for other peptides such as 8–26 fragment of melittin [27] and bombolitin [15]. In the region where the peptide assumes a maximal molecular packing, the surface potential changed from ~500 mV on pure water to ~370 mV on saline solution subphases.

The ranges of collapse pressure and the surface potential values found for MP1 have been assigned to α-helical peptides [15] such as bombolitin III [28] and LL-37 [29] which also form stable monolayers at the air–water interface. In this regard, a mostly α-helical structure is expected for Polybia-MP1 arranged in a monolayer since this is its preferred structure when adsorbed to zwitterionic (PC) and anionic vesicles (PC/PG 7:3) showing 83% and 85% of helical content as determined by circular dichroism, respectively [13]. The peptide is hydrophilic with a mean residue hydrophobicity $\langle H \rangle = -0.11$ and a hydrophobic moment per residue $\mu = 0.29$, which characterizes a surface helical peptide [30]. The μ value for MP1 is most likely responsible for the interfacial activity of the peptide at the air–water interface. Assuming an α-helical structure, the expected organization of the peptide adopting this structure is shown as an inset in Fig. 1B.

The mean molecular areas for MP1 at low and high surface pressure on water were 200 Å^2 (at 5 mN/m) and 160 Å^2 (at 15 mN/m), while on 150 mM NaCl, these values shifted to 280 Å^2 (5 mN/m) and 250 Å^2 (15 mN/m). In order to get an insight on the possible orientations

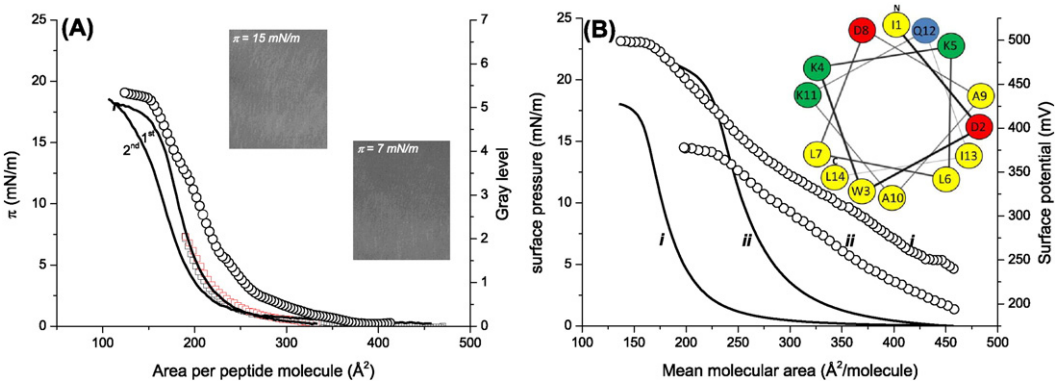

Fig. 1. (A) Pressure–area compression isotherms of Polybia-MP1. Left scale: first and second compression isotherms for MP1 monolayer on pure water. The first compression–expansion–recompression cycle was performed up to 8 mN/m (open squares: red represents compression and black expansion) and above π_{col} (continuous line). Right scale: Evolution of the gray level of images obtained with BAM (open circles). The insets show representative BAM images of films composed of pure peptide on water at the indicated surface pressures. The gray levels were rescaled from the original 0–255 range to 0–40 for better visualization. (B) Surface pressure–mean molecular area (continuous line) and surface potential–mean molecular area (open circle) compression isotherms for films composed of MP1 spread on water (i) or 150 mM NaCl, pH 7.4 (ii). The inset shows a wheel representation of the peptide in an α-helix configuration (green represents positively charged; red, negatively charged; blue, polar uncharged and yellow, hydrophobic residues). All isotherms were registered at $T = 20$ °C.

acquired by the peptide at the interface, an estimation of the area occupied by an α-helical segment with the helix axis oriented parallel and perpendicular to the interface was performed as follows: the theoretical area occupied by an α-helical segment with the helix axis oriented parallel to a surface may be estimated as 15 Å (the helix diameter considering the side chains [31]) times 1.5 Å (length per amino acid) = 22.5 Å^2. Then, for a segment of 14 residues, the area would be 22.5 Å^2 × 14 ≈ 315 Å^2. On the other hand, the theoretical area of an α-helix oriented perpendicular to the interface assuming an average helical diameter mentioned above would be approximately 177Å^2 ($\pi \times 7.5^2$ Å^2). Comparing these values with the experimental mean molecular area, we suggest that the axis of the helix was oriented mainly perpendicular to the air–water and air–NaCl solution interfaces for coherent monolayers, as previously reported for other peptides such as Aurein 2.3 [32] Maculatin and Citropin [31]. A higher average molecular area for the peptides onto NaCl solutions, together with a lower surface potential suggest that the tilting of the molecules were different when salt was present in the subphase.

The surface potential is a complex parameter whose value results from the contribution of the molecular dipole/multipoles, the hydration water and the ions at the interface. The decrease of the surface potentials in salt subphase compared to water may be due to distinct orientations of the molecular multipoles (both, from charged residues and from the bonds of the peptide backbone) at these subphases and/or to the reorientation of water molecules plus the potential generated by the ionic double layer, since the peptide at this pH has local charges and also a net charge. All these factors contribute to the observed surface potential value in a very complex manner, and therefore it is not possible to assess from these results the precise orientation of the peptide at each condition, and whether it was oriented with the carboxylic or the amino terminus pointing to water, or half population with each orientation.

In summary, the compression isotherms of MP1 indicated that the peptide had significant interface activity, in concordance to its amphipathic character. The peptide adopted mostly α-helical structure at the interface, with its axis oriented nearly normal to the surface. The behavior of the peptide films depended on the subphase ionic strength, suggesting a role played by electrostatic interactions. When the peptide charges were not screened, the MP1 films were more compact and the molecules were able to get closer to each other indicating the presence of favorable electrostatic interactions within the film.

3.2. Peptide–DPPC isotherms on pure water and saline solution interfaces

The compression isotherms (π vs A) of DPPC co-spread with various amounts of MP1 in a range between 2.4 and 7.2 mol% are shown in Fig. 2A. In these plots, the area corresponds to the average area per lipid (without considering the amount of added peptide) for better visualizing the effect of the presence of the peptide on the isotherm of DPPC.

The compression isotherm for pure DPPC film at the air–water interface showed the typical behavior, with a phase transition from liquid-expanded (LE) to liquid-condensed (LC) state at ~4 mN/m (π_t) as previously reported [33]. The addition of increasing amounts of the peptide to the lipid films induced an increase in the lift-off area/phospholipid molecule, a slight increase in the values of the transition pressure, π_t (see Fig. 3A), and the appearance of second plateau at about 18 mN/m (close to the collapse pressure of pure MP1 films, see Fig. 1). At a surface pressure of ~40 mN/m the mean molecular areas showed the same values than those of pure lipid films, suggesting that the peptide was squeezed out from the film. This was confirmed by performing compression and decompression cycles, which showed a significant area shifts, indicating that the peptide was expelled to the subphase at these surface pressures (data not shown).

At pH 7.4 and 150 mM NaCl the π-A isotherm of pure DPPC was slightly displaced to higher molecular areas than those observed at the air–water interface (Fig. 2B) due to the presence of ions in the aqueous phase [34]. In this interface, increasing amounts of peptide did not alter the π_t values (see Fig. 3A). A second plateau was also observed in the presence of the peptide on saline solutions at values of the surface pressure corresponding to the collapse of pure peptide films on similar subphases (~21 mN/m). The superposition of the isotherms at pressures above 40 mN/m suggests that the peptide was also being squeezed out to the subphase in the air–NaCl solutions interfaces.

From the compression isotherms of the mixed films, the mean molecular areas at fixed surface pressure was obtained and plotted as a function of the mole percentage of peptide in Fig. 3B and C. Note that for these calculations the mean area/molecule was recalculated considering the number of total molecules at the interface (lipid and peptide). On pure water, positive deviations from ideality were observed at all the analyzed surface pressures, indicating that peptide–lipid interactions are less attractive than peptide–peptide and lipid–lipid interactions, and also indicating that there was mixing of the components, at least partially. This is in agreement with the trend followed by π_t (Fig. 3A), which slightly increased in the presence of MP1 indicating a partial mixing of the peptide with the phospholipid on water. An increase in the π_t also indicates a preferential mixing of the peptide with the lipid in the LE phase, thereby stabilizing this phase in detriment of the LC phase.

In saline conditions, no deviation was observed from the additivity rule, suggesting ideal miscibility or total immiscibility. Ideal miscibility is however highly unlikely considering the different size and properties of the peptide compared to the lipid molecules. Furthermore, as already indicated the presence of peptide did not alter the transition pressure of DPPC on 150 mM NaCl subphases (Fig. 3A), indicating that the peptide

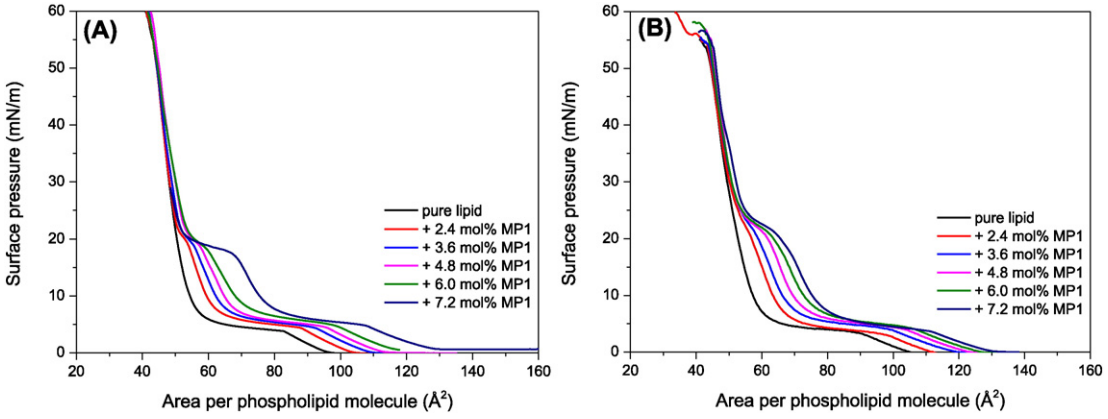

Fig. 2. Surface pressure–area compression isotherms for DPPC films co-spread with increasing amounts of MP1 onto a water surface (A) or 150 mM NaCl, pH 7.4 (B). The areas correspond to the total monolayer area normalized by the amount of lipids (without considering the peptide).

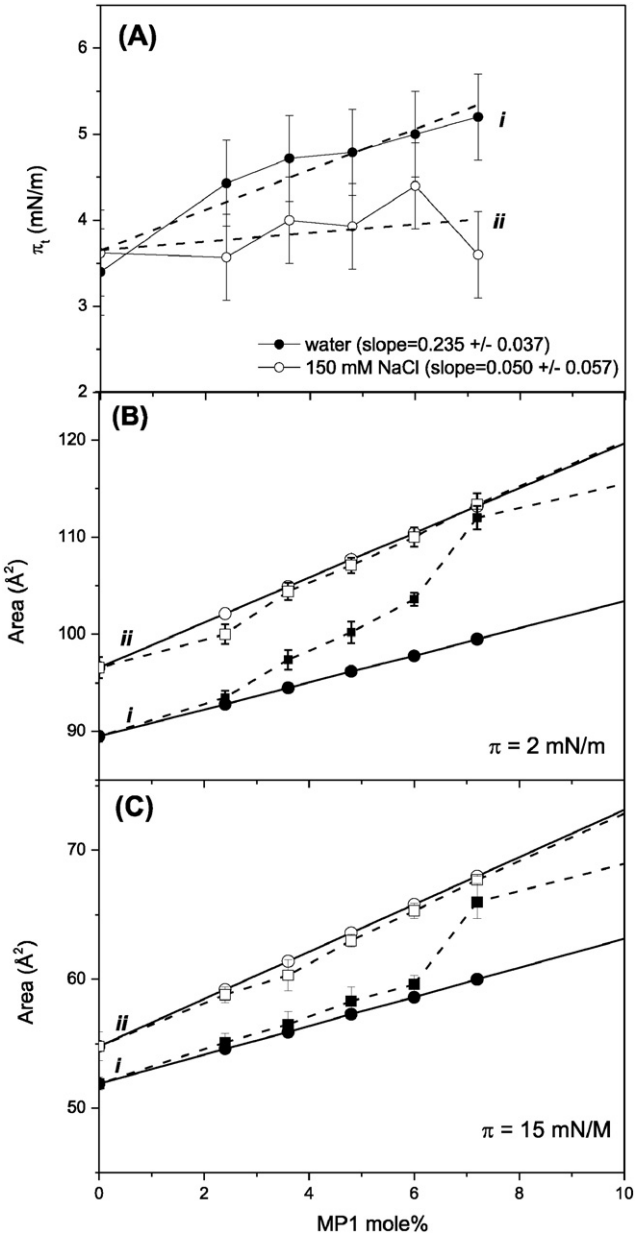

Fig. 3. (A) Surface pressure corresponding to the DPPC phase transition as a function of the molar fraction of the peptide. The dashed line corresponds to a linear fit and the error of the data points corresponds to the resolution of the technique (~0.5 mN/m). (B) and (C) Mean molecular areas as a function of the molar fraction of the peptide for the studied monolayers at different surface pressures: (B) π = 2 mN/m and (C) π = 15 mN/m. The average value ± the standard deviation of at least 3 independent measurements are depicted. Continuous lines correspond to mean molecular area of an ideal mixture and the dashed line to the real area. The subphases correspond to pure water (i) and 150 mM NaCl, pH 7.4 (ii) in all cases.

did not mix with DPPC in the LE or LC phases, or that the energy of mixing is similar with both phases, thereby inducing no change in the π_t value. This last hypothesis is again highly unlikely considering the different features of MP1 and DPPC molecules, further suggesting complete immiscibility of these molecules on 150 mM NaCl subphases.

3.3. Domain morphology of DPPC/MP1 monolayers determined by BAM and AFM at different ionic strengths

The morphological features of the lipid phase transition and the changes induced by the peptide on the domain formation in the presence and absence of salt were studied by BAM. On pure water, pure DPPC film showed the characteristic domains with "triskelion" shapes with different gray levels (Fig. 4), in agreement with data reported in the literature [35]. Nucleation occurred at ~4 mN/m, and further compression led to domain growth until the whole monolayer was covered by lipid in the LC phase state.

When 7.2 mol% of MP1 was co-spread with DPPC on the air–water interface, LC nucleation occurred at higher surface pressure (in agreement with the changes in the π_t values), and the domains showed more branched structures, with longer and more curved arms compared to those in the absence of the peptide (Fig. 4). The areas occupied by the thinner phase (darker regions in the BAM images) at comparable surface pressures were always higher in the presence of MP1, further indicating that the peptide mixed with preference in the LE phase. This phenomenon was also observed at MP1 proportions as low as 2.4 mol%, though in a less marked fashion (see Fig. S1 in Supplementary material).

The resolution of the BAM technique did not allow us to describe the structure of the nuclei and feature center of the domains; therefore, mixed films were transferred to glass surfaces at 15 mN/m and scanned by AFM as described in the experimental section. At this pressure, the peptide was still not expulsed to the subphase and a good transfer of the film was possible. Fig 5 shows the obtained AFM images. At low amplifications (Fig. 5A), the transferred film showed elongated domains with similar features as those observed at the air–water interface by BAM. Higher amplifications showed that the center of the domains also exhibited elongated arms (Fig. 5B and C).

BAM images were also obtained for mixed films compressed on 150 mM NaCl, pH 7.4 (Fig. 6). At these conditions, the formation of LC domains occurred at the same surface pressure than in the absence of peptide, in agreement with the data shown in Fig. 3A. The shape of the domains on saline solutions was very similar to those observed in the absence of the peptide, i.e. the presence of the peptide did not perturb domain nucleation and growth. At surface pressures higher than 24 mN/m, domains fused and the whole film became LC. For films composed of pure lipid, this occurred at lower surface pressure (~11 mN/m).

Comparison of the images with and without peptide at similar surface pressures indicate that the peptide most probably remained in the less dense region (darker gray regions in the BAM images), since this region occupied larger areas in the presence of MP1. To better quantify this effect, the percentage of each region (darker and lighter gray regions) was calculated from images as those in Fig. 6 and plotted as a function of the surface pressure in Fig. 7. This figure shows that the percentage of the darker region (DR) decreased and the percentage of lighter region (LR) increased as the film was compressed, as expected. In the presence of peptide, the DR area was larger than those occupied by the LE phase in pure lipid films at comparable surface pressures, up to a value of ~22 mN/m, which correspond to the pressure where the peptide was squeezed out to the subphase. This result indicates that the peptide was located in the DR together with the lipid in the LE phase, thereby increasing the amount of these regions but without mixing with the lipid; otherwise the π_t value would change (but it remained constant, see Fig. 3A) and the mean molecular area most probably would deviate from the ideal line (but it showed ideal behavior, see Fig. 3B and C).

In order to test whether the peptide was totally absent in the LC phase on saline solutions, we calculated the percentage of area that would occupy the lipid at 15 mN/m using the mean molecular area from the compression isotherms of pure DPPC on NaCl solutions (Fig. 2B), which according to Fig. 3C is a good approximation since the area of the mixture showed an ideal behavior. The results and the details for this calculation are shown in Table 1. The comparison of the data obtained from the images (Fig. 7) and the data calculated as explained suggest that the LC domains were composed of nearly pure DPPC, while the darker regions corresponded to mostly pure MP1 at 15 mN/m. The calculated area occupied by the lipids was slightly larger than the area occupied by the LR, and therefore some lipid molecules

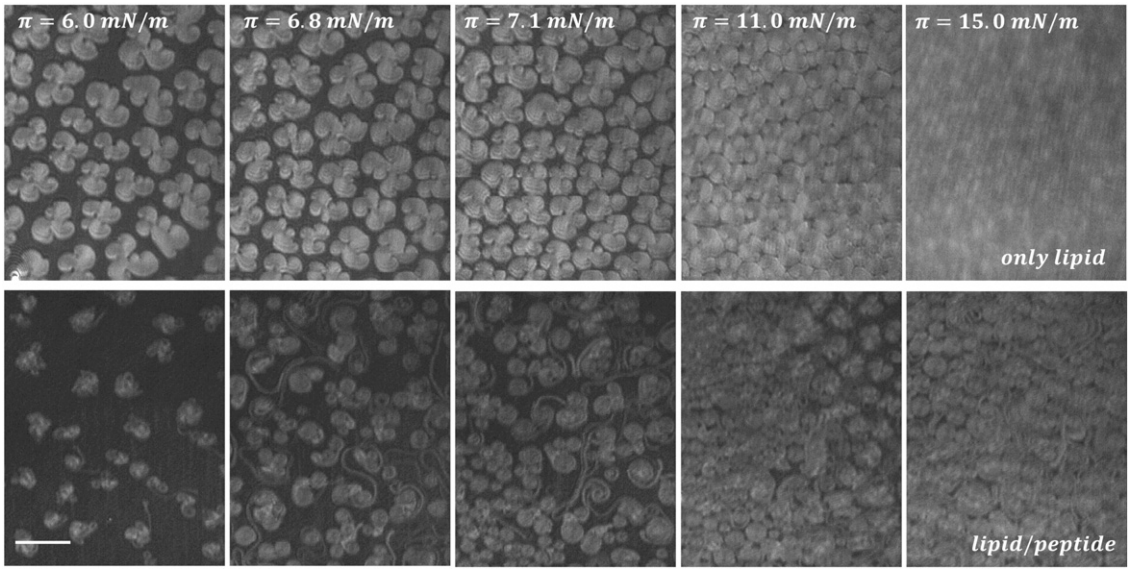

Fig. 4. Representative BAM images for monolayers composed of DPPC (top panels) or DPPC/MP1 for $X_{MP1} = 0.072$ (bottom panels) spread on pure water and registered during compression at 20 °C and at the indicated surface pressures. Scale bars correspond to 50 μm.

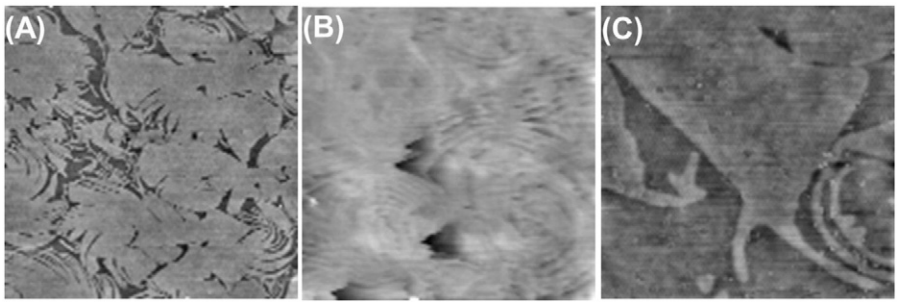

Fig. 5. Representative AFM topographic images for DPPC/MP1 films ($X_{MP1} = 0.072$) transferred to a glass coverslip from the air–water interface at 15 mN/m. Image size: 50×50 μm^2 (A), 20×20 μm^2 (B) and 8.6×8.6 μm^2 (C).

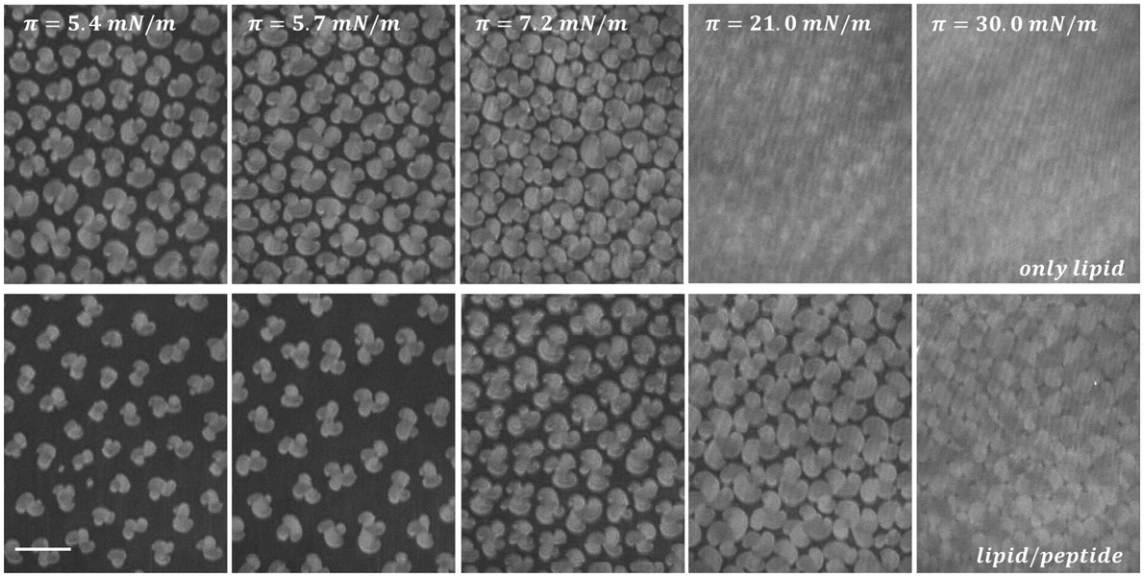

Fig. 6. Representative BAM images for monolayers composed of DPPC (top panels) or DPPC/MP1 for $X_{MP1} = 0.072$ (bottom panels) spread on 150 mM NaCl, pH 7.4 and registered during compression at 20 °C and at the indicated surface pressures. Scale bar corresponds to 50 μm.

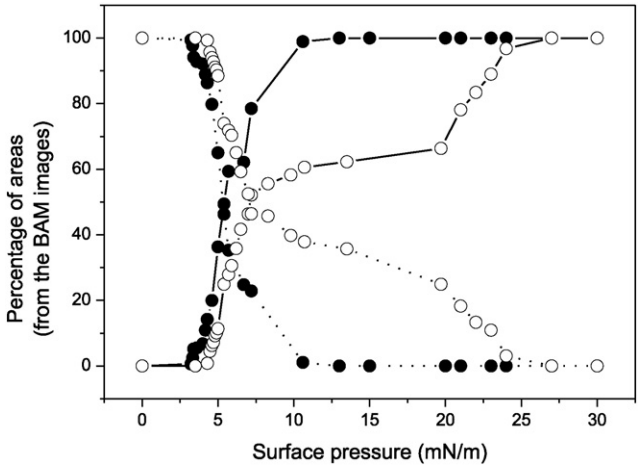

Fig. 7. Percentage of area occupied by the lighter gray region (continuous line) or by the darker gray region (dashed line) as a function of the surface pressure determined from the BAM images of films composed of pure lipid (close circles) and lipid/peptide mixtures (open circles) spread on 150 mM NaCl, pH 7.4.

remained with the peptide in the DR until it was expelled to the subphase.

Similar calculations were performed for films spread on pure water, using images as those in Fig. 4 and the mean molecular areas of the isotherms of pure DPPC at 15 mN/m on water (Fig. 2A). The determination of the percentages from the images is not so precise in this case, since the domain branches are very thin, which hinders the generation of a binary image. Furthermore, in this case, using the mean molecular area of the isotherm of the pure lipid introduces an error since the mixing involved expansion of the components as shown in Fig. 3B and C, but it allows getting an insight of the difference in composition of the lighter and darker regions with those on NaCl solutions. The results are shown in Table 1, and indicate that at these conditions, domains incorporate peptide, since the lipid alone occupied smaller areas than those corresponding to the LR.

With the aim of determining whether the effect promoted by the salt on the DPPC domain shape was due to charge screening, the domains morphology was investigated by BAM (Fig. 8) under increasing amounts of NaCl. In films composed of pure DPPC, the addition of 0.1 or 1 mM NaCl to the subphase showed no effects on the films properties. However, in the case of DPPC–MP1 films, increasing amounts of salt in the subphase affected the domain morphology, being the domain shapes less branched as the amount of salt increased. The presence of 7.2 mol% of MP1 on films of DPPC on subphases containing 0.1 mM NaCl partially induced the formation of branched domains, resembling those observed on water with smaller amounts of peptide (Fig. S1 in Supplementary material).

Table 1
Percentage of area occupied by the different regions, calculated area occupied by each molecule, and amount of domains at each condition.

Condition	BAM images		[b]% lipid area	[c]Number of domains
	[a]Lighter grey regions	[a]Darker grey regions		
pH 7.4, 150 mM NaCl	65 ± 1	35 ± 1	71	63 ± 7
Water	88 ± 2	12 ± 2	69	–
pH 2.0, 150 mM NaCl	54 ± 2	48 ± 2	60	184 ± 12
pH 4.0, 150 mM NaCl	63 ± 4	37 ± 4	79	170 ± 15
pH 10.0, 150 mM NaCl	70 ± 2	30 ± 2	72	60 ± 5

[a] Percentage of area occupied by the lighter and the darker grey phases of BAM images at 15 mN/m. The data represents the average ± the standard deviation of at least 5 images.
[b] Percentage of area occupied by the lipids calculated as: $\%A_L = x_L MMA_L / MMA_T \times 100$, where x_L is the molar fraction of the lipid in the mixture, MMA_L is the mean molecular area of the pure lipid (from the corresponding compression isotherm at 15 mN/m) and MMA_T is the mean molecular area of the mixed film (area of the trough at 15 mN/m divided by the amount of seeded molecules).
[c] Number of domains in 50,000 μm^2 determined from BAM images at 6–8 mN/m and at each condition.

Important roles played by the anion on the film topography has been previously reported [34]. Therefore, with the purpose of evaluate whether the effect of salt was derived from specific interactions or merely electrostatic screening, experiments were performed using NaBr solution instead of NaCl. Increasing amounts of NaBr were added to the subphase and films composed of pure lipid or lipid + 7.2 mol% MP1 were observed by BAM while compressing (Fig. S2 in Supplementary material). The obtained images showed that NaBr led to films with similar features to those on NaCl at the same salt concentration, indicating that salt effects were derived from non-specific charge screening.

In the case of domains composed by a fluid phase, many studies indicated that the shape of the domains is determined by a competition between the line tension and the dipole moment difference between the LE and the domain phases, and that flower-like shapes are acquired for domains larger than a critical radius [36]. In this work, domains were rigid, without visible shape relaxation during the experiments (minutes), and the AFM images showed that domains acquire a branched-like shape from the first stages of domain growth, and not just once a critical radius was reached (Fig. 5B and C). For rigid domains, Krüger and Lösche introduced a third term in the domain free energy accounting for oriented intermolecular interactions that predicts a curved domain shape [37]. Their model indicates that electrostatic repulsion between the molecules inside the domain is not enough for the development of elongated domain formation. Curled domains with a preferential orientation of growth only appear if the molecules adopt preferential orientations inside the domain as it grows. Considering this latter we suggest that as the domains grow on pure water subphases, they incorporate both, DPPC and MP1, each of them with a preferred orientation, leading to very thin arms with preferential directions of growth.

The possible attractive electrostatic interactions between peptide molecules are those generated between the anionic aspartic acid residues (D2 and D8) and the cationic lysines (K4, K5 and K11). When the film is still not coherent, at high mean molecular areas (higher than the lift-off) these residues may be screened by the presence of NaCl or NaBr. An increase of the salt concentration increases the probability of counter-ions binding to the charged residues, leading to a gradual increase in the amount of neutralized peptides via ion-pair formation and thereby decreasing the peptide–peptide attractive interactions. Once the film becomes coherent, the accessibility of the subphase ions to the charged residues probably decreases. In order to assess if the interaction between ions and peptides was possible during the whole compression process or only when the peptides are far from each other the following experiment was performed. Films of MP1 were prepared on water and compressed up to 3 or 15 mN/m. Once one of these lateral pressures was reached, the value was maintained with the constant pressure mode of the Langmuir balance and 5 mL of NaCl 6 M were added to the subphase (180 mL total volume) with a microsyringe leading to a subphase concentration of ~160 mM. Measurements of the area at constant surface pressure showed negligible changes (similar to those of a control where 5 mL of pure water was added to the subphase), indicating that the ions from the subphase were not able to penetrate the interface and screen the charged residues once the film was coherent, and therefore, no increase in the mean molecular area was observed after the saline solution was added (data not shown).

From all the results showed so far, we propose that the attractive interactions observed between the peptide molecules on water at neutral pH are related to salt bridges between the pairs D2–K4/K5 and D8–K11 if all the peptides lie with the same orientation at the interface, or between the pairs D2 - K11 and D8 - K4/K5 if the peptides adopt antiparallel orientation. Only when these salt bridges are formed between the peptides, MP1 mixes with DPPC thereby suggesting that a specific peptide–peptide arrangement is necessary for the development of

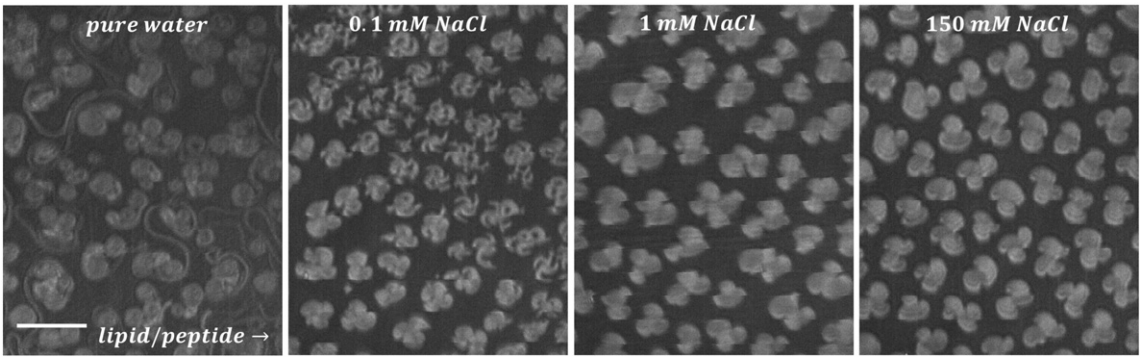

Fig. 8. Representative BAM images for monolayers composed of DPPC/MP1 ($X_{MP1} = 0.072$) spread on solutions of increasing NaCl concentrations at 20 °C and at 7–8 mN/m. Scale bar corresponds to 50 μm.

favorable lipid–peptide interactions. Our hypothesis is that when the peptides are close together, these residues with opposing charges induce preferential orientations of the molecules in the crystal when the domains grow. Each new peptide in the growing domains will attach preferentially with its negative residues to a peptide that exposes the positive residues thereby generating domains with branched shapes.

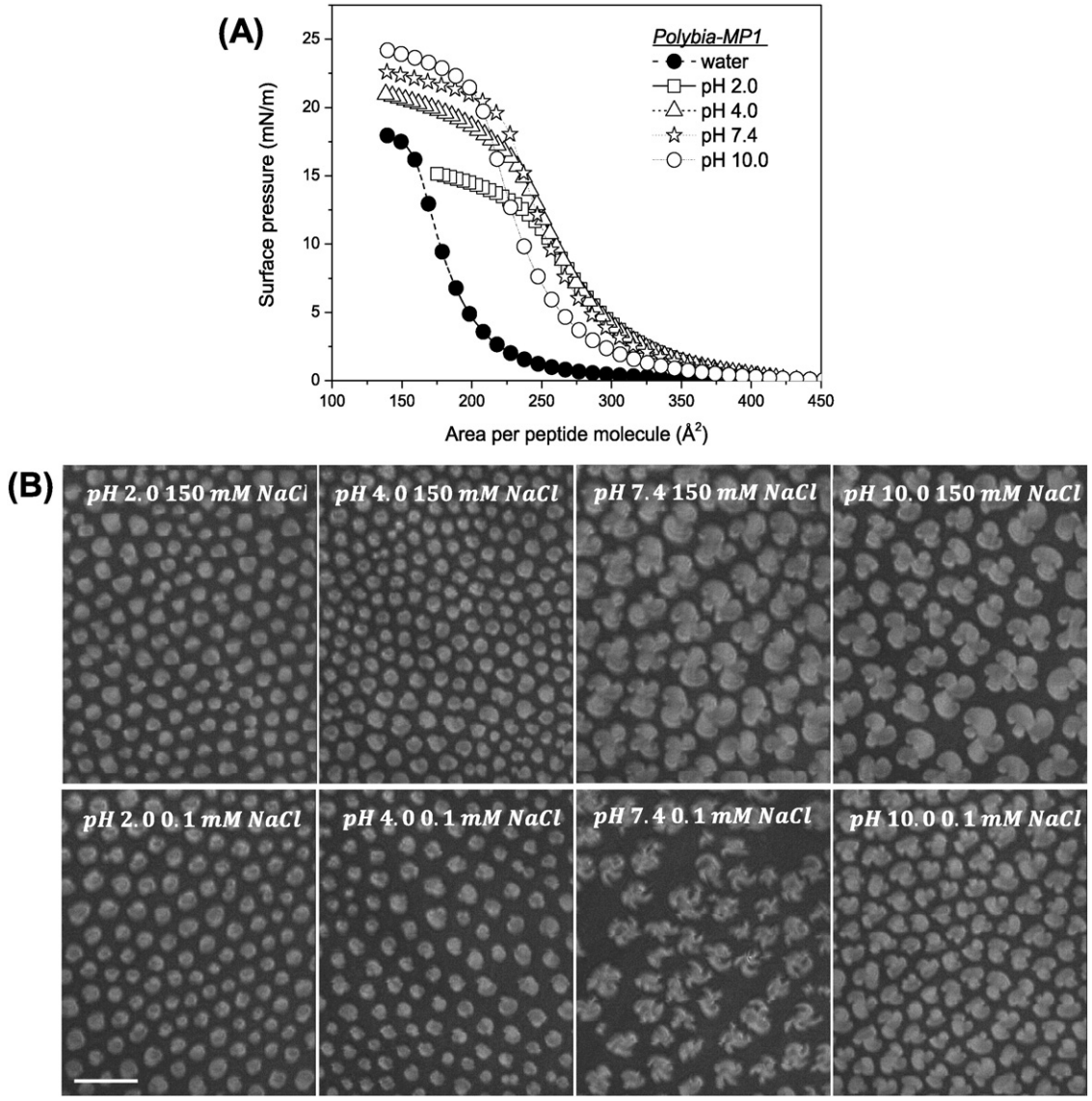

Fig. 9. (A) Compression isotherms of films composed of pure MP1 on water (same curve than in Fig. 1A) and on 150 mM NaCl subphases of the indicated pHs. (B) Representative BAM images of monolayers composed of DPPC/MP1 ($X_{MP1} = 0.072$) spread on NaCl solution at the indicated concentrations and pHs, registered during compression at 20 °C and at 7–8 mN/m. Scale bar corresponds to 50 μm.

With this peptide–peptide arrangement, the hydrophobic regions of the peptide remain available for favorable hydrophobic DPPC–peptide interactions (see the position of the yellow residues in the inset of Fig. 1B). At this point it is important to remark that, still in the presence of the peptides, the domains keep the preferential orientations of the curled arms, indicating that even when the domains are a mixture of DPPC and MP1, the chiral DPPC–DPPC interactions remain, as previously observed for a DPPC/copolymer mixture [38].

On 150 mM NaCl solutions and pH 7.4, the charged residues bonded to counter-ions when the peptide was at high mean molecular areas, and the counter-ions remained attached to the peptide when the film became coherent. As a consequence of the ion binding, the interaction between the aspartic acids and the lysines were no longer so strong, leading to a less attractive total free energy of peptide–peptide interaction and thus, the peptide remained in the less dense phase when mixed with DPPC, where they were able to occupy larger molecular areas. An increase in the salt concentration (from 0.1 mM to 150 mM) translates to a decrease in the proportion of free charged residues (not bonded to counter-ions), and lead to a gradual decrease in the attractive interactions between peptides with a concomitant decrease in the peptide–lipid mixing ability.

3.4. Peptide isotherms and domain morphology of DPPC/MP1 monolayers on solution of acidic and basic pHs

According to our hypothesis, if the charges of the aspartic acid or the lysine residues are neutralized, the total attractive interactions will decrease, and the peptides would accumulate in the darker regions when mixed with DPPC and form films with mean molecular areas higher than on water when pure, independent of the ionic strength.

Therefore, we analyzed the impact of the presence of the peptide on the phase behavior of DPPC monolayer at acidic and basic pHs with different ionic strength. Fig. 9 shows the compression isotherms of pure MP1 (A) in the presence of 150 mM NaCl together with images of mixed films obtained by BAM (B) at each pH and salt conditions.

At pH 2 and 4, a more repulsive peptide–peptide interaction profile prevailed, as evidenced by larger mean molecular areas compared to water (Fig. 9A). This effect was independent on the ionic strength (not shown). Furthermore, at these conditions the domains showed more rounded shapes (see images in Fig. 9B) than at all other conditions. The comparison of the percentage of the areas for DR and LR with the calculated area occupied by the lipids (using the mean molecular areas of the isotherms of pure lipid at each condition, which are not shown) suggest that the peptide remained in the darker region and that the domains were composed of nearly pure lipid in the LC phase state (Table 1).

At pH 10, the peptide was partially deprotonated and, similar to films on acid subphases, the LR was composed of almost pure lipid and the DR was mostly peptide (Table 1). Additionally, the areas occupied by the pure peptide were larger than on water (Fig. 9A) and independent on the ionic strength (not shown). In summary, the behavior of the pure and mixed films at acid and basic pHs are in agreement with the proposed hypothesis.

As already commented, on acid subphases the domains were smaller and more rounded than at basic and at neutral pHs with high ionic strength (see Fig. 9B). This correlated with a higher number of domains at acidic pHs (see Table 1), and thus with a higher domain nuclei when nucleation occurred. It was previously reported that as the nuclei density increases, the capture area of each domain decreases, leading to smaller and more rounded domains [39]. In a system with a classical nucleation process, the amount of nuclei increases as the perturbation rate in relation to the diffusion in the system increases. This implies that the amount of domains is expected to be higher as the compression rate increases or as the lipid diffusion decreases (i.e. as the viscosity of the film increases). Following this, we suggest that in the analyzed systems, films of DPPC and MP1 at low pHs (with total or partial deprotonation of aspartic acidic) may be more viscous than at neutral pHs (net charge +2) and basic pHs (with partial deprotonation of the lysines). However, this is just a hypothesis and the surface viscosity has to be determined in order to completely explain the topography on acidic solutions.

4. Conclusion

In the present study, we analyzed the surface properties of the peptide Polybia-MP1 and its interaction with DPPC in Langmuir monolayer. Polybia-MP1 presented a significant interfacial activity on both, water and ionic subphases, forming stable monolayers. The lateral areas and surface potential values obtained from compression isotherms suggested that the peptide adopted a mostly helical structure in agreement with results of the peptide adsorbed to anionic liposomes [13], with its axis oriented almost perpendicular to the air–water interface.

The peptide occupied larger areas at comparable surface pressures at all conditions different from water, suggesting that the peptide–peptide interactions were more attractive in the absence of salt and at neutral pHs. On pure water, DPPC and MP1 co-crystallized forming domains with branched shapes, while on subphase with high salt concentrations (1 mM or higher) or on acidic or basic solutions (independent of the ionic strength), the peptide was excluded from the regions of the denser phase and the domains presented “triskelion-like” shapes, similar to those formed by pure DPPC films. Therefore, at those conditions the peptides were not able to get close to each other suggesting that the peptide–peptide interactions become less attractive than on pure water. In order to explain the decrease in the total attractive interaction, we propose that salt bridges between the aspartic acids and the lysines may form on water, thus allowing the peptides to get closer to each other, and also to co-crystallize with the lipid molecules. These salt bridges would be less stable on acidic subphases, because the aspartic acids are partially neutralized and on basic solutions because the lysines are partially neutralized. At neutral pHs with high ionic strength, counter-ions partially neutralize both kinds of charged amino acids, and the formation of the salt bridges is less favored than on pure water.

The new results shown here highlight the importance of the aspartic acid residues in the peptide–peptide and peptide–lipid interactions, which is in line with previous results where an important role was assigned to the D2 residue in the modulation of the membrane-MP1 interactions [11,13]. According to the results shown here, the peptide–lipid interaction are regulated by the peptide–peptide electrostatic attractions, probably as a consequence of the formation of a particular peptide arrangement, in which the hydrophobic regions are exposed to the lipids and the charged residues to the neighboring peptides. In order to form this supramolecular structure, the counter-ions have to be displaced from peptides by the charged residues of neighboring peptides, in other words, the counter-ions compete with the peptides for the aspartic acids and the lysines of the peptides.

This particular surface arrangement may explain the higher affinity to anionic vesicles found for MP1 compared to higher positive charged peptides [12]. To the long range peptide-membrane electrostatic attraction, a short range interaction (the establishment of peptide–peptide salt bridges) is added for this peptide, stabilizing the peptide residence in the lipid membrane.

In summary, we described here the possible lateral interactions of MP1, when the peptide formed pure films and also when mixed with a lipid. We found a complex electrostatic regulation of the peptide–peptide interactions and thereby of the pure and mixed film properties. In this system, the balance between attractive electrostatic interactions and total attractive and repulsive interactions may be finely tuned by the aqueous ionic strength and pH. The results shown here for MP1 may be very probably extrapolated to other pore forming peptides with similar sequences.

Transparency document

The Transparency document associated with this article can be found, in online version.

Acknowledgments

The authors acknowledge the financial support from São Paulo Research Foundation (J.R.N. grant # 2011/11640-5), FONCyT-Argentina (PICT 0344) and SECyT-Univ. Nacional de Córdoba. D.S.A has a PhD fellowship (FAPESP, grant # 2012/08147-8). We also would like to acknowledge CEMETRO (UTN, Córdoba, Argentina) and Drs. D. Brusa and C. Schurrer for the AFM determinations. J.R.N. is researcher of CNPq. N.W. and M. L. F. are researchers of CONICET.

Appendix A. Supplementary data

Supplementary data to this article can be found online at http://dx.doi.org/10.1016/j.bbamem.2015.12.010.

References

[1] M.R. Yeaman, Mechanisms of antimicrobial peptide action and resistance, Pharmacol. Rev. 55 (2003) 27–55.
[2] M. Dathe, H. Nikolenko, J. Meyer, M. Beyermann, M. Bienert, Optimization of the antimicrobial activity of magainin peptides by modification of charge, FEBS Lett. 501 (2001) 146–150.
[3] Y. Chen, C.T. Mant, S.W. Farmer, R.E.W. Hancock, M.L. Vasil, R.S. Hodges, Rational design of alpha-helical antimicrobial peptides with enhanced activities and specificity/therapeutic index, J. Biol. Chem. 280 (2005) 12316–12329.
[4] L.T. Nguyen, E.F. Haney, H.J. Vogel, The expanding scope of antimicrobial peptide structures and their modes of action, Trends Biotechnol. 29 (2011) 464–472.
[5] S.E. Blondelle, K. Lohner, M. Aguilar, Lipid-induced conformation and lipid-binding properties of cytolytic and antimicrobial peptides: determination and biological specificity, Biochim. Biophys. Acta 1462 (1999) 89–108.
[6] D.W. Hoskin, A. Ramamoorthy, Studies on anticancer activities of antimicrobial peptides, Biochim. Biophys. Acta Biomembr. 1778 (2008) 357–375.
[7] B.M. Souza, M.A. Mendes, L.D. Santos, M.R. Marques, L.M.M. César, R.N.A. Almeida, et al., Structural and functional characterization of two novel peptide toxins isolated from the venom of the social wasp *Polybia paulista*, Peptides 26 (2005) 2157–2164.
[8] K. Wang, B. Zhang, W. Zhang, J. Yan, J. Li, R. Wang, Antitumor effects, cell selectivity and structure–activity relationship of a novel antimicrobial peptide polybia-MPI, Peptides 29 (2008) 963–968.
[9] K. Wang, J. Yan, B. Zhang, J. Song, P. Jia, R. Wang, Novel mode of action of polybia-MPI, a novel antimicrobial peptide, in multi-drug resistant leukemic cells, Cancer Lett. 278 (2009) 65–72.
[10] M.P. Dos Santos Cabrera, M. Arcisio-Miranda, R. Gorjão, N.B. Leite, B.M. De Souza, R. Curi, et al., Influence of the bilayer composition on the binding and membrane disrupting effect of polybia-MP1, an antimicrobial mastoparan peptide with leukemic T-lymphocyte cell selectivity, Biochemistry 51 (2012) 4898–4908.
[11] N.B. Leite, L.C. Da Costa, D. Dos Santos Alvares, M.P. Dos Santos Cabrera, B.M. De Souza, M.S. Palma, et al., The effect of acidic residues and amphipathicity on the lytic activities of mastoparan peptides studied by fluorescence and CD spectroscopy, Amino Acids (2011).
[12] M.P. Dos Santos Cabrera, S.T.B. Costa, B.M. De Souza, M.S. Palma, J.R. Ruggiero, J. Ruggiero Neto, Selectivity in the mechanism of action of antimicrobial mastoparan peptide Polybia-MP1, Eur. Biophys. J. 37 (2008) 879–891.
[13] N.B. Leite, D. dos Santos Alvares, B.M. de Souza, M.S. Palma, J. Ruggiero Neto, Effect of the aspartic acid D2 on the affinity of Polybia-MP1 to anionic lipid vesicles, Eur. Biophys. J. (2014).
[14] R. Koynova, M. Caffrey, Phases and phase transitions of the phosphatidylcholines, Biochim. Biophys. Acta Rev. Biomembr. 1376 (1998) 91–145.
[15] R. Maget-Dana, The Monolayer Technique: A Potent Tool for Studying the Interfacial Properties of Antimicrobial and Membrane-lytic Peptides and Their Interactions With Lipid Membranes, Biochim. Biophys. Acta - Biomembr. 1999, pp. 109–140.
[16] N. Wilke, Chapter Two — Lipid Monolayers at the Air–Water Interface: A Tool for Understanding Electrostatic Interactions and Rheology in Biomembranes, Adv. Planar Lipid Bilayers Liposomes 2014, pp. 51–81.
[17] A. Clausell, M.A. Busquets, M. Pujol, A. Alsina, Y. Cajal, Polymyxin B-lipid interactions in Langmuir–Blodgett monolayers of *Escherichia coli* lipids: a thermodynamic and atomic force microscopy study, Biopolymers 75 (2004) 480–490.
[18] S.R. Dennison, L.H.G. Morton, A.J. Shorrocks, F. Harris, D.A. Phoenix, A study on the interactions of Aurein 2.5 with bacterial membranes, Colloids Surf. B Biointerfaces 68 (2009) 225–230.
[19] A. Hinz, H.-J. Galla, Viral membrane penetration: lytic activity of a nodaviral fusion peptide, Eur. Biophys. J. 34 (2005) 285–293.
[20] S. Ali, J.M. Smaby, H.L. Brockman, R.E. Brown, Cholesterol's interfacial interactions with galactosylceramides, Biochemistry 33 (1994) 2900–2906.
[21] B. Caruso, A. Mangiarotti, N. Wilke, Stiffness of lipid monolayers with phase coexistence, Langmuir 29 (2013) 10807–10816.
[22] A. Mangiarotti, N. Wilke, Energetics of the phase transition in free-standing versus supported lipid membranes, J. Phys. Chem. B 119 (2015) 8718–8724.
[23] F.V. Mercado, B. Maggio, N. Wilke, Phase diagram of mixed monolayers of stearic acid and dimyristoylphosphatidylcholine. Effect of the acid ionization. Chem. Phys. Lipids 164 (2011) 386–392.
[24] B.R. Malcolm, The Structure and Properties of Monolayers of Synthetic Polypeptides at the Air–Water Interface, Prog. Surf. Membr. Sci. 1973, pp. 183–229.
[25] R. Volinsky, S. Kolusheva, A. Berman, R. Jelinek, Investigations of antimicrobial peptides in planar film systems, Biochim. Biophys. Acta Biomembr. 1758 (2006) 1393–1407.
[26] K.S. Birdi, Self-assembly Monolayer Structures of Lipids and Macromolecules at Interfaces, Springer Science & Business Media, 2006.
[27] V.S. Gevod, K.S. Birdi, Melittin and the 8-26 fragment. Differences in ionophoric properties as measured by monolayer method. Biophys. J. 45 (1984) 1079–1083.
[28] G. Signor, S. Mammi, E. Peggion, H. Ringsdorf, A. Wagenknecht, Interaction of bombolitin III with phospholipid monolayers and liposomes and effect on the activity of phospholipase A2, Biochemistry 33 (1994) 6659–6670.
[29] F. Neville, M. Cahuzac, O. Konovalov, Y. Ishitsuka, K.Y.C. Lee, I. Kuzmenko, et al., Lipid headgroup discrimination by antimicrobial peptide LL-37: insight into mechanism of action, Biophys. J. 90 (2006) 1275–1287.
[30] D. Eisenberg, E. Schwarz, M. Komaromy, R. Wall, Analysis of membrane and surface protein sequences with the hydrophobic moment plot, J. Mol. Biol. 179 (1984) 125–142.
[31] E.E. Ambroggio, F. Separovic, J. Bowie, G.D. Fidelio, Surface behaviour and peptide–lipid interactions of the antibiotic peptides, maculatin and citropin, Biochim. Biophys. Acta Biomembr. 1664 (2004) 31–37.
[32] M. Mura, S.R. Dennison, A.V. Zvelindovsky, D.A. Phoenix, Aurein 2.3 functionality is supported by oblique orientated α-helical formation, Biochim. Biophys. Acta, Biomembr. 1828 (2013) 586–594.
[33] M. Dyck, A. Kerth, A. Blume, M. Lo, Interaction of the Neurotransmitter, Neuropeptide Y, With Phospholipid Membranes: Infrared Spectroscopic Characterization at the Air/Water Interface, 22152–221592006.
[34] A. Aroti, E. Leontidis, E. Maltseva, G. Brezesinski, Effects of hofmeister anions on DPPC Langmuir monolayers at the air–water interface, J. Phys. Chem. B 108 (2004) 15238–15245.
[35] R.M. Weis, H.M. McConnell, Two-dimensional chiral crystals of phospholipid, Nature 310 (1984) 47–49.
[36] D.J. Keller, H.M. McConnell, V.T. Moy, Theory of superstructures in lipid monolayer phase transitions, J. Phys. Chem. 90 (1986) 2311–2315.
[37] P. Krüger, M. Lösche, Molecular chirality and domain shapes in lipid monolayers on aqueous surfaces, Phys. Rev. E Stat. Phys. Plasmas Fluids Relat. Interdiscip. Topics 62 (2000) 7031–7043.
[38] P. Scholtysek, S.W.H. Shah, S.S. Müller, R. Schöps, H. Frey, A. Blume, et al., Unusual triskelion patterns and dye-labelled GUVs: consequences of the interaction of cholesterol-containing linear-hyperbranched block copolymers with phospholipids, Soft Matter 11 (2015) 6106–6117.
[39] F. Vega Mercado, B. Maggio, N. Wilke, Modulation of the domain topography of biphasic monolayers of stearic acid and dimyristoyl phosphatidylcholine, Chem. Phys. Lipids 165 (2012) 232–237.